

VEX: Photoproduction of Excited Vector Mesons

GLUEX Collaboration

Abstract

Elastic photoproduction should be ideal for studying the excitations (V^*) of the vector mesons. Although there is general agreement about the existence of the corresponding excited isovector-vector mesons ($\rho(1450)$ and $\rho(1700)$), the excited isoscalar-vector mesons ($\omega(1420)$ and $\omega(1650)$) and the excited isoscalar-vector with hidden strangeness ($\phi(1680)$), measurements of the masses, widths and decay modes are inconsistent. Much of the information in hand comes from experiments studying e^+e^- collisions with only a few results from experiments studying hadro- or photo-production. We propose to search for and measure the masses, widths and decay modes of these excited vector states in the reaction $\gamma p \rightarrow V^* p$. The proposed experiment (VEX) will use a bremsstrahlung photon beam produced with 6 GeV electrons. The detector consists of a 3-cm LH₂ target, charged particle tracking and electromagnetic calorimetry around and downstream of the target and a time-of-flight system. The experiment will focus on final states containing a recoil proton and some combination of mesons leading to neutral energy in the calorimeter and/or two additional charged particles.

Physics motivation

Why study the photoproduction of excited light quark vector mesons? First of all, in both the light and heavy quark sectors the ground vector mesons ($1^3S_1 \bar{q}q$), the ρ , ω , ϕ , J/ψ and Υ are well understood. From a study of their decays in ϕ , J/ψ and Υ factories much has been learned about QCD hadronic physics. The ground state light quark vector nonet is very well understood. The flavorless members of this nonet, the ω and ϕ , are nearly ideally mixed so that ϕ is essentially composed entirely of s quarks and the ω entirely of u and d quarks. Within the quark model we expect excitations of the ground state vectors and these include both radial (2^3S_1) excitations and orbital (1^3D_1) excitations. In the heavy quark sector these vector excitations are well mapped and studied. But the situation in the light quark sector is at best murky, as will be discussed below. An understanding of how the light quark and heavy quark sectors connect is important if we are to eventually understand the light quark sector in mapping gluonic excitations – *glueballs* and *hybrid* mesons. The vector mesons are thus ideal for providing this connection.

In the heavy quark sector the vectors are produced in e^+e^- collisions. In the light quark sector much of the information we have on possible excited vector states also comes from e^+e^- collisions. But the measurements of the masses, widths and decay modes of reported states are inconsistent. Photoproduction is complementary to e^+e^- collisions and may be better suited to understanding the light quark excited vectors. One advantage of producing states directly in e^+e^- collisions is that one starts with a clean $J^{PC} = 1^{--}$ initial state but a disadvantage is that the mass reach is limited for any given collider. Photoproduction does not suffer from this limitation. On the other hand photoproduction allows for other J^P states. This could be viewed as a virtue since it allows one to exploit interference with well-known states to help establish new states.

The elastic photoproduction of the ground state vector mesons, ρ , ω and ϕ has been well studied. Within the Vector Dominance (VDM) picture the photon fluctuates into a virtual $1^3S_1 \bar{q}q$ (vector meson V) that elastically scatters off of the proton resulting in $\gamma p \rightarrow Vp$. Of course the photon can also fluctuate into a virtual 2^3S_1 or $1^3D_1 \bar{q}q$ (excited vector V^*) followed elastic scattering of the excited vector resulting in $\gamma p \rightarrow V^*p$.

Our current information about the excited vector mesons comes from e^+e^- collisions with only a few results from hadro- and photo-production and τ decays [5]. There is general agreement about the existence of these excited isovector-vector mesons ($\rho(1450)$ and $\rho(1700)$), the excited isoscalar-vector mesons ($\omega(1420)$ and $\omega(1650)$) and the excited isoscalar-vector with hidden strangeness ($\phi(1680)$). There are, however, inconsistencies in the masses, widths and decay modes. For example, the quoted masses for the $\rho(1450)$ range from 1290 ± 40 to 1582 ± 25 MeV/ c^2 while the quoted widths range from 60 ± 15 to 547 ± 86 MeV/ c^2 . Masses and widths for the other excited vector states show similar inconsistencies. Many of the decay modes allowed by quantum number conservation are merely listed as *seen* in the Review of Particle Physics (RPP) [5]. The 2004 RPP has a review [6] of the $\rho(1450)$ and $\rho(1700)$. In the 1988 version of the RPP there was a single excited ρ – the $\rho(1600)$ which has been superseded by the $\rho(1450)$ and $\rho(1700)$. There is also a report of a $\bar{K}K$ state reported at a mass of 1750 MeV/ c^2 [7] by the FOCUS collaboration. Whether this state is the same as $\phi(1680)$ or another excitation is an open question.

Separately, and with co-workers, A. Donnachie has reviewed the experimental situation with excited vector mesons [8, 9, 10, 11]. The disparity among various experiments with regard to the properties

Table 1: Decay modes of the excited vector mesons accessible to VEX. Dominant decay enclosed in brackets.

$\rho(1450)$	$\rho(1700)$	$\omega(1420)$	$\omega(1650)$	$\phi(1680)$
$\pi\pi$	$\pi\pi$	–	–	–
e^+e^-	e^+e^-	e^+e^-	e^+e^-	e^+e^-
–	K^+K^-	–	–	K^+K^-
4π	$[\rho\pi\pi]$	$\omega\pi\pi$	$\omega\pi\pi$	$[K^*K]$
–	$\rho\eta$	–	$\omega\eta$	–
–	$\omega\pi$	$[\rho\pi]$	$\rho\pi$	–

of excited vector mesons, alluded to above, highlights why these states are of great interest. Further experiments are needed to learn about the substructure of these states. A comparison of e^+e^- data, τ decays and photoproduction is essential.

Table 1 lists the decay modes of the excited vector mesons accessible to VEX. In addition to the states already reported it will be essential to search the entire mass region up to about 1.8 GeV/ c^2 , which is the near the limit of the mass reach of VEX.

The final states available to VEX include decay modes of the ground state vectors ρ , ω and ϕ . The elastic photoproduction of these states has been well measured, including at VEX energies – at 2.8 and 4.7 GeV [1], at 4.3 GeV [2], from 6.5 to 17.8 GeV [3], and at 16 GeV [4]. Comparison of production (*e.g.* t dependence) and decay (*e.g.* check of s-channel helicity conservation) characteristics with published results will be important validation for VEX. The dominant decays are $\rho \rightarrow \pi^+\pi^-$, $\omega \rightarrow \pi^+\pi^-\pi^0$ and $\phi \rightarrow K^+K^-$ and $\phi \rightarrow \pi^+\pi^-\pi^0$. All three ground state vector mesons have decays into e^+e^- , $\mu^+\mu^-$ and $\pi^0\gamma$ and the decay $\phi \rightarrow \eta\gamma$ is also accessible.

There are also other important cross checks. For example the $\pi^+\pi^-$ mode is allowed for vectors but $\pi^0\pi^0$ is not. The $\rho^\pm\pi^\mp$ mode is allowed for isovectors but the $\rho^0\pi^0$ is not.

Experiment overview

A schematic of the apparatus is shown in Figure 1 and the detector specifications are summarized in Table 3. The major components include a 3-cm LH₂ target, tracking drift chambers (D1-D3) downstream of the target and around the target (CDC), time-of-flight scintillator wall (TOF), a lead glass electromagnetic calorimeter (LGD) downstream of the target and an electromagnetic calorimeter (BCAL) surrounding the target. There is no magnetic field. Events selected for analysis will require identification of a recoil proton using at least D1 and dE/dx and TOF. In addition to the recoil proton topologies of two charged particles and/or neutral particles will be identified using kinematic constraints. Charged particle directions will be determined assuming the event vertex is in the target with other track points determined by D1-D3 and TOF. VEX will be sensitive to final states listed in Table 2. Details regarding the reconstruction technique and acceptances for various final states are presented in the Appendix.

Table 2: Final states to be measured by VEX. We assume the detection of the recoil proton. Final states with only charged particles will require no energy in the LGD or the γ -GUARD. Final states with all neutrals recoiling against the proton will use veto information from D1-D3. Strangeness conservation will also be imposed in the kinematic identification.

Final State	Detectors used and/or other comments
$\pi^+\pi^-p$	Use D1-D3 and TOF
$\pi^0\pi^0p$	Use LGD and $\pi^0 \rightarrow 2\gamma$
$\pi^0\eta p$	Use LGD and $\pi^0 \rightarrow 2\gamma$ and $\eta \rightarrow 2\gamma$
K^+K^-p	Use D1-D3 and TOF
e^+e^-p	Use D1-D3 and TOF and LGD
$\mu^+\mu^-p$	Use D1-D3 and TOF and LGD
$\pi^+\pi^-\pi^0p$	Use D1-D3 and TOF and LGD: $\pi^0 \rightarrow 2\gamma$
$K^+K^-\pi^0p$	Use D1-D3 and TOF and LGD: $\pi^0 \rightarrow 2\gamma$
$\rho^0\pi^0p$ or $\rho^\pm\pi^\mp p$	$\rho^0 \rightarrow \pi^-\pi^+$ or $\rho^\pm \rightarrow \pi^\pm\pi^0$
$\rho^0\eta p$	$\rho^0 \rightarrow \pi^-\pi^+$ and $\eta \rightarrow 2\gamma$
$\omega\pi^0p$ or $\omega\eta p$	$\omega \rightarrow \pi^0\gamma$
$\phi\pi^0p$ or $\phi\eta p$	$\phi \rightarrow K^+K^-$
$K^\pm K^{*\mp}p$	$K^{*\mp} \rightarrow K^\mp\pi^0$

Table 3: Detector element specifications

Detector Element	Size	Resolution
μ BCAL	Cylinder, id=50cm length=150 cm thickness=15 cm	$\sigma(z) = 3cm$ $\sigma(\phi) = 0.038$ $\frac{\sigma}{E} = \frac{0.04}{\sqrt{E(GeV)}}$ $E_{min} = 25MeV$
μ CDC	Cylinder, id=45cm length =150 cm thickness = 4 cm	$\sigma(R\phi) = 150\mu m$ $\sigma(z) = 150\mu m / \sin(10^\circ)$
D1	Radius = 56 cm	$\sigma_x = \sigma_y = 0.1cm$
D2	Radius = 72 cm	$\sigma_x = \sigma_y = 0.1cm$
ToF	Square, 250 cm	$\sigma_t = 70ps$ $\sigma_x = \sigma_y = 6cm/\sqrt{12}$
LGD	Radius =106 cm	$\sigma_x = \sigma_y = 0.7cm/\sqrt{E(GeV)}$ $\frac{\sigma}{E} = \frac{0.08}{\sqrt{E(GeV)}} + 0.035$ $E_{min} = 100MeV$

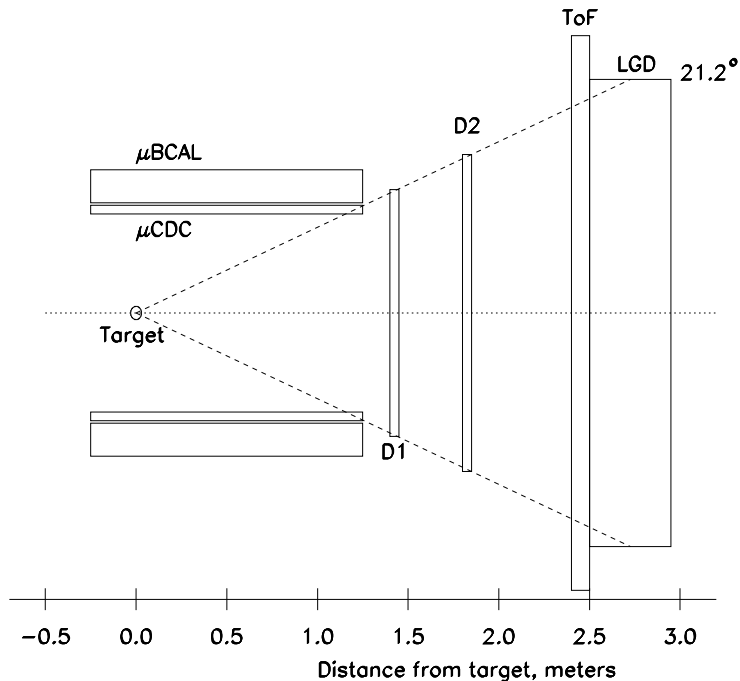


Figure 1: Schematics of the VEX experiment.

The acceptance in effective mass for the modes: $\pi^+\pi^-$, K^+K^- , $\pi^0\pi^0$ and $\pi^+\pi^-\pi^0$ is shown in Figure 2. The acceptance includes both geometry and the requirement that the event be reconstructed. The acceptance in the Gottfried-Jackson angles: θ and ϕ for the modes: $\pi^+\pi^-$, K^+K^- , $\pi^0\pi^0$ and $\pi^+\pi^-\pi^0$ are shown in Figure 3. Note that the acceptances for the $\pi^+\pi^-$ and K^+K^- are very similar. The π^0 mass resolution for (i) both photons in the LGD; (ii) one photon in BCAL and the other in the LGD; and (iii) both photons in BCAL is shown in Figure 4.

The tagged photon beam will have a flux of $10^7 \gamma/s$ – a conservative flux to insure association of an event with the photon that initiated it. At this flux, with a 3-cm LH_2 target, a $1 \mu\text{b}$ cross-section leads to 1.2 ev/s. The total interaction rate will be 150 Hz. To set the scale, the ρ elastic cross section is $15 \mu\text{b}$ and the ϕ elastic cross section is $0.5 \mu\text{b}$.

Appendix: Event Reconstruction

Consider reactions of the type

$$\gamma p \rightarrow M^+ M^- p \quad (1)$$

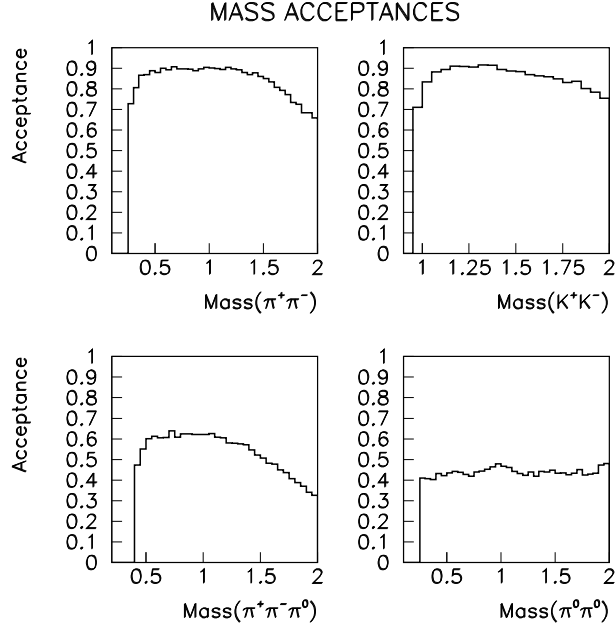


Figure 2: The acceptance in effective mass for the modes: $\pi^+\pi^-$, K^+K^- , $\pi^0\pi^0$ and $\pi^+\pi^-\pi^0$.

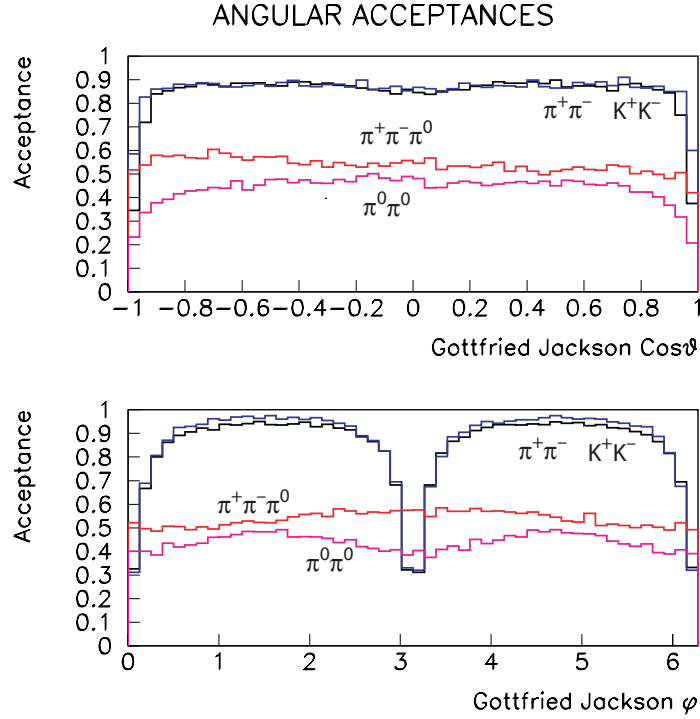


Figure 3: The acceptance in the Gottfried-Jackson angles: (top) θ and (bottom) ϕ for the modes: $\pi^+\pi^-$, K^+K^- , $\pi^0\pi^0$ and $\pi^+\pi^-\pi^0$. Note that the acceptances for the $\pi^+\pi^-$ and K^+K^- are very similar.

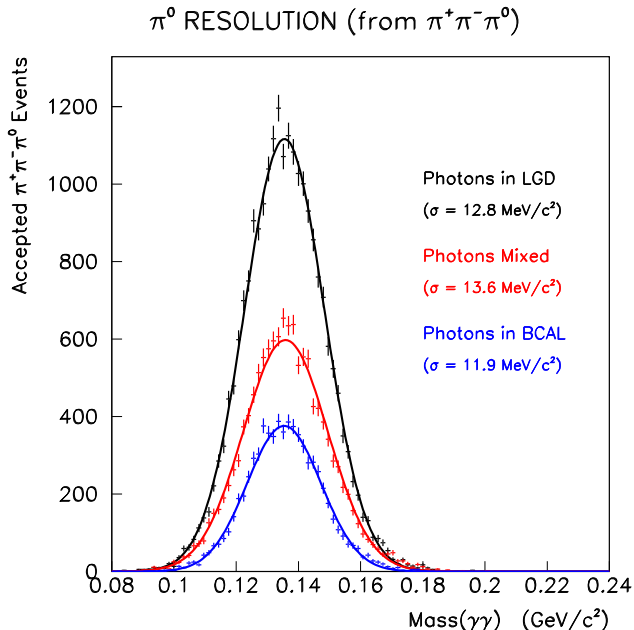


Figure 4: The π^0 mass resolution for (i) both photons in the LGD; (ii) one photon in BCAL and the other in the LGD; and (iii) both photons in BCAL.

Conservation of momentum determines the magnitudes of the three charged particles in the final state from measurements of their directions. If all tracks are constrained to pass through the origin of coordinates (taken as the center of the target) these directions are measured by finding a single point on a track. Denote a point on a track as (x_i, y_i, z_i) . Then

$$\begin{pmatrix} p_{ix} \\ p_{iy} \\ p_{iz} \end{pmatrix} = p_{iz} \begin{pmatrix} x_i/z_i \\ y_i/z_i \\ 1 \end{pmatrix} \quad (2)$$

with

$$\begin{pmatrix} p_{z1} \\ p_{z2} \\ p_{z3} \end{pmatrix} = \begin{pmatrix} x_1/z_1 & x_2/z_2 & x_3/z_3 \\ y_1/z_1 & y_2/z_2 & y_3/z_3 \\ 1 & 1 & 1 \end{pmatrix}^{-1} \begin{pmatrix} 0 \\ 0 \\ p_{beam} \end{pmatrix}. \quad (3)$$

The ratios of coordinates appearing in equations 2 and 3 are slopes of tracks. If the position of a charged particle is measured at more than one point in space, a fit can be performed to improve the knowledge of these ratios.

Again, using the constraint that all particles are produced at the center of the target the momentum of a photon in the final state is fully determined by the LGD. The direction is determined geometrically from the observed position of the electromagnetic shower in the calorimeter, the magnitude of the momentum is determined by the energy of the observed cluster.

Charged particle momenta from reactions of the type

$$\gamma p \rightarrow n\gamma M^+ M^- p \quad (4)$$

are reconstructed by replacing equation 3 with

$$\begin{pmatrix} p_{z1} \\ p_{z2} \\ p_{z3} \end{pmatrix} = \begin{pmatrix} x_1/z_1 & x_2/z_2 & x_3/z_3 \\ y_1/z_1 & y_2/z_2 & y_3/z_3 \\ 1 & 1 & 1 \end{pmatrix}^{-1} \left[\begin{pmatrix} 0 \\ 0 \\ p_{beam} \end{pmatrix} - \sum^n \vec{p}_\gamma \right]. \quad (5)$$

Reconstruction is complete when a mass is assigned to each track. This assignment is trivial for the photons and achieved with time of flight measurements and/or dE/dX measurements in other detector elements.

Equation 3 (or equivalently Eq. 5) clearly imply VEX is limited to at most three charged particles in the final state. Implicitly assumed in Eq. 5 is that all final state particles are observed.

The resolution achievable by this reconstruction technique clearly depends on the resolution achievable on the position measurements and on the performance of the LGD. Implicit in the above is that all particles are produced at the center of the target. To achieve an acceptable approximation to this, the beam must have a small transverse extent and the target must be longitudinally thin.

References

- [1] J. Ballam et al. *Phys. Rev. D*, 5:545, 1972.
- [2] Y. Eisenberg et al. *Phys. Rev. Lett.*, 22:669, 1969.
- [3] W. Jones et al. *Phys. Rev. Lett.*, 21:586, 1968.
- [4] M. Davier et al. *Phys. Lett. B*, 28:619, 1969.
- [5] S. Eidelman et al. *Phys. Lett. B*, 592:1, 2004.
- [6] S. Eidelman et al. The $\rho(1450)$ and $\rho(1700)$ by S. Eidelman and J. Hernandez. *Phys. Lett. B*, 592:576, 2004.
- [7] R. Mitchell. U. of Tennessee Dept. of Physics Ph. D. Thesis.
- [8] A. Donnachie, 2001. hep-ph/0106197.
- [9] A. Donnachie and Yu. S. Kalashnikova, 2001. hep-ph/0110191.
- [10] A. Donnachie, 1991. Invited talk at Hadron '91 - U. of Maryland.
- [11] A. Donnachie and A. B. Clegg. *Nucl. Phys. B (Proc. Suppl.)*, 21:118, 1991.
- [12] D. C. Fries et al. *Nucl. Phys. B*, 143:408, 1978.
- [13] L. Bibrzycki, L. Lesniak, and A. Szczepaniak. *Eur. Phys. J. C*, 34:335, 2004.